Module- 5 : Introduction to Hydrostatic Units (Pumps and Motors)

Lecture: 22 Gear Type Hydrostatic Unit-I Analysis of a Gear Pump

(Continued from Lecture 20).

Introduction: In earlier lecture the derivation of flow rate in a gear pump is established. In this lecture the detail calculation and design procedure will be presented.

Mesh Geometry

Coordinate Systems. Schematics of the gear tooth mesh are shown in Figs. 3 and 4. X-Y is the fixed Cartesian coordinate system. It is oriented by a fixed angle ξ with the line joining the centres of the gear. ξ will be determined later. Whereas x-y is the rotating coordinate system which is fixed to the left gear. It is so chosen that while the tooth mesh begins the x coordinate passes through the midline of the driving (left) gear tooth in contact. The rotation x-y defined by θ_1. At θ_1 is equal to 0, X and x axes coincide.

Instantaneous Point of Tooth Contact. The instantaneous point of tooth contact, which always lies on the line of action, can be defined in polar coordinates by radius ρ_1 and angle β_1 with respect to x-y coordinate system. The equation of the line of action with respect to x-y coordinate system is expressed as (Fig. 4),

$$\hat{y}\sin(\alpha+\theta_1-\xi)=1-\hat{x}\cos(\alpha+\theta_1-\xi) \tag{11}$$

From the gear geometry- $r_{b_1}=r_{p_1}\cos(\alpha)$.

The tooth contact point- $x=\rho_1\cos(\beta_1)$ and $y=-\rho_1\sin(\beta_1)$.

Substituting these in equation (11) and rearranging the contact point is defined as,

$$\hat{\rho}_1=\sec(\alpha+\beta_1+\theta_1-\xi). \tag{12}$$

Again from the geometry of the involute tooth profile β_1 is defined as,

$$\beta_1=\psi_1-\sqrt{\hat{\rho}_1^2-1}+\cos^{-1}\left(\frac{1}{\hat{\rho}_1}\right). \tag{13}$$

Where $\psi_1=\pi/(2Z_1)$.

Equations (12) and (13) must be solved numerically for a given θ_1.

Starting Mesh Position. Referring to Fig.-3 the starting tooth contact point can be defined in polar coordinate as,

$$\hat{\rho}_{1_s}=\sqrt{\hat{l}_s^2+\hat{r}_{p_1}^2-2\hat{r}_{p_1}\hat{l}_s\sin(\alpha)} \tag{14}$$

Where the starting length of action is expressed as,

$$\hat{l}_s = \sqrt{\hat{r}_{a_2}^2 - \hat{r}_{p_2}^2 \cos(\alpha)} - \hat{r}_{p_2} \sin(\alpha). \tag{15}$$

Also, from equation (13),

$$\beta_{1_s} = \psi_1 - \sqrt{\hat{\rho}_{1_s}^2 - 1} + \cos^{-1}\left(\frac{1}{\hat{\rho}_{1_s}}\right). \tag{16}$$

Now, ξ can be derived with respect to the starting contact point parameters, as,

$$\xi = \beta_{1_s} + \sin^{-1}\left(\frac{\hat{l}_s \cos(\alpha)}{\rho_{1_s}}\right).$$

Instantaneous Length of Action From geometry in fig 4 instantaneous length of action can be determined as fallows

$$\sin(\xi - \beta_1 - \theta_1) = \hat{l}\cos\alpha / \hat{\rho}_1$$

$$\hat{l} = \hat{\rho}_1 \ \text{Sin}(\xi - \beta_1 - \theta_1) \sec\alpha \tag{17}$$

The relationship between ρ_1 and β_1 is nonlinear hence a numerical solution to these equations will yield the most accurate results for instantaneous length of action however, a closed-form approximation to these solutions is adopted here.

Closed Form Approximation:- For generating a closed form solution for the instantaneous pump flow, a Taylor series expansion of Eq. (17) may be taken for small values of θ_1. Taylor series expansion yields the following result

$$\hat{l} = \hat{\rho}_{1_s} \text{Sin}(\xi - \beta_{1_s} - \theta_1) \sec\alpha - \hat{\rho}_{1_s} \cos(\xi - \beta_{1_s}) \sec(\alpha)\theta_1$$

$$\hat{l} = \hat{l}_s - \hat{\rho}_{1_s} \cos(\xi - \beta_{1_s}) \sec(\alpha)\theta_1 \tag{18}$$

For better approximation assume $\hat{\rho}_{1_s} \cos(\xi - \beta_{1_s}) \sec\alpha = 1$

Then the equation (18) will reduce to,

$$\hat{l} = \hat{l}_s - \theta_1 \tag{19}$$

The error with this approximation may be found by subtracting Eq (19) from Eq (17) i.e

$$\varepsilon = \hat{\rho}_1 \sin(\xi - \beta_1 - \theta_1) \sec\alpha - \hat{l}_s + \theta_1. \tag{20}$$

This error is zero for θ_1 **=0** but increases slightly as θ_1 increases.

Pump Flow Characteristics The general form of Eq (10) will be used to describe the flow characteristics of the pump. From Eq. (10) it can be shown that the maximum flow output of the pump will occur when l^2 is minimum and min $\hat{l}^2$ =0. Therefore,

$$\hat{Q}_{\text{dmax}} = \tfrac{1}{2}\{ \hat{r}_{a_1}^2 + \hat{r}_{a_2}^2 (\hat{r}_{p1} / \hat{r}_{p2}) - \hat{r}_{p1} (\hat{r}_{p1} + \hat{r}_{p2}) \} \tag{21}$$

Similarly, the minimum flow output of pump occurs when l^2 is maximum. Since maximum $\hat{l}^2 = \hat{l}_s^2$, the minimum pump flow rate is given by

$$\hat{Q}_{\text{d min}} = ½\{\ \hat{r}_{a_1}^2 + \hat{r}_{a_2}^2 (\hat{r}_{p1}/\hat{r}_{p2}) - \hat{r}_{p1}\ (\hat{r}_{p1}+\hat{r}_{p2}) - (1+\hat{r}_{p1}/\hat{r}_{p2})\ \hat{l}_s^2\} \qquad (22)$$

The amplitude of the flow pulse is then given by

$$\Delta\hat{Q}_{\text{d}} = \hat{Q}_{\text{d max}} - \hat{Q}_{\text{d min}} = ½\ (1+\hat{r}_{p1}/\hat{r}_{p2})\ \hat{l}_s^2 \qquad (23)$$

The average flow rate for one flow pulsation is given by

$$\hat{Q}_{\text{d avg}} = \frac{1}{\hat{l}_s - \hat{l}_f}\int_{\hat{l}_f}^{\hat{l}_s} \hat{Q}_d\, d\hat{l} = ½\{\ \hat{r}_{a_1}^2 + \hat{r}_{a_2}^2 (\hat{r}_{p1}/\hat{r}_{p2}) - \hat{r}_{p1}\ (\hat{r}_{p1}+\hat{r}_{p2}) - \hat{m}\} \qquad (24)$$

Where l_s is the length of action when mating teeth just touch, and l_f is the length of action that occurs just prior to another set of teeth making contact within the mesh and 'm' is given as

$$\hat{m} = (1+\hat{r}_{p1}/\hat{r}_{p2})\ \{(\hat{l}_s + \hat{l}_f)^2 - \hat{l}_s\,\hat{l}_f\}/3 \qquad (25)$$

Theoretical Pump Design Usually the teeth numbers of driver and driven gear are same in common gear pumps. However, pumps with equal as well as different numbers of gear teeth are considered for the purposes of comparing and finding the optimum flow ripple characteristics. To make a clear comparison among pumps of different teeth pairs, the average flow rate of each pump is maintained constant in the design process. In other words, Eq. (24) is held constant for all pump designs. In this equation, the result of closed form approximation is used for evaluation of pump design i.e.

$\hat{l} = \hat{l}_s - \theta_1$ is substituted in the pump flow equation.

The starting length of action $\hat{l}_s$ is defined in equation (15). The final length of action $\hat{l}_f$ is derived following equation (17), as-

$$\hat{l}_f = \hat{\rho}_{1_f} \sin(\xi - \theta_{1_f} - \beta_{1_f}) \sec(\alpha), \qquad (26)$$

Where,

$$\hat{\rho}_{1_f} = \sec(\alpha + \beta_{1_f} + \theta_{1_f} - \xi),$$

$$\beta_{1_f} = \psi_1 - \sqrt{\hat{\rho}_{1_f}^2 - 1} + \cos^{-1}\left(\frac{1}{\hat{\rho}_{1_f}}\right), \qquad \} \qquad (27)$$

$$\theta_{1_f} = \frac{2\pi}{Z_1} \text{ and } \psi_1 = \frac{\pi}{2Z_1}.$$

The pitch radius of each gear is determined from the following geometric relation from the fundamental law of gearing.

$$r_{b1} = r_{p1}\cos\alpha,\ 1 = r_{p1}\cos\alpha\ /\ r_{b1},\quad \hat{r}_{p1} = \sec\alpha,\ \hat{r}_{p2} = (Z_2/Z_1)\ \hat{r}_{p1} \qquad \} \qquad (28)$$

The addendum radius of each gear is designed according the American Gear Manufacturing Association (AGMA) recommended standards. These recommendations are given as

$$\hat{r}_{a_1} = \frac{2+Z_1}{Z_1}\hat{r}_{p1},\ \hat{r}_{a_2} = \frac{2+Z_2}{Z_2}\hat{r}_{p2} \qquad \} \qquad (29)$$

By selecting the number of teeth on each gear (Z_1 and Z_2), specifying the average flow rate of the pump (Eq. (24)) ($\hat{Q}_{d_{avg}}$ =0.297) and enforcing the constraints of

Eqs. (26) to (29), the pressure angle α is solved numerically. Results are tabulated in Table 1.

Numerical Results and discussion:

Centre Distance and Physical Pump Size The centre distance in dimensionless form is given by

$$\hat{A} = \hat{r}_{p1} + \hat{r}_{p2}. \tag{30}$$

The centre distance can be used to gauge the physical sizes of pumps for same volume displacement (swept volume). It was observed that the centre distance increases strongly as the number of teeth on the driven gear increases and decreases weakly as the number of teeth on the driving gear increases. This result says that physically smaller pumps (of the same displacement per revolution) may be designed if the number of teeth on the driven gear is decreased while the number of teeth on the driving gear is increased. Figure 5 shows a plot of the centre distance as it varies with tooth number on both the driving and driven gears in dimensionless form.

Z_1	Z_2	r_{p1}	r_{p2}	$A=r_{p1}+r_{p2}$
13	12	1.021	.942	1.96
13	13	1.022	1.022	2.04
13	14	1.023	1.102	2.13
13	15	1.025	1.182	2.21
13	**16**	1.025	1.262	2.29
14	8	1.031	.589	1.62
14	13	1.039	.965	2.00
14	14	1.041	1.041	2.08
14	**15**	1.042	1.116	2.16
14	16	1.042	1.191	1.76
15	12	1.061	.849	1.91
15	13	1.062	.921	1.98
15	**14**	1.063	.992	2.06
15	15	1.064	1.064	2.13
15	16	1.065	1.136	2.20
16	12	1.088	.817	1.90
16	**13**	1.089	.885	1.97
16	14	1.090	.954	2.04
16	15	1.091	1.023	2.11
16	16	1.091	1.091	2.18

Table: 1 design with identical average flow rates

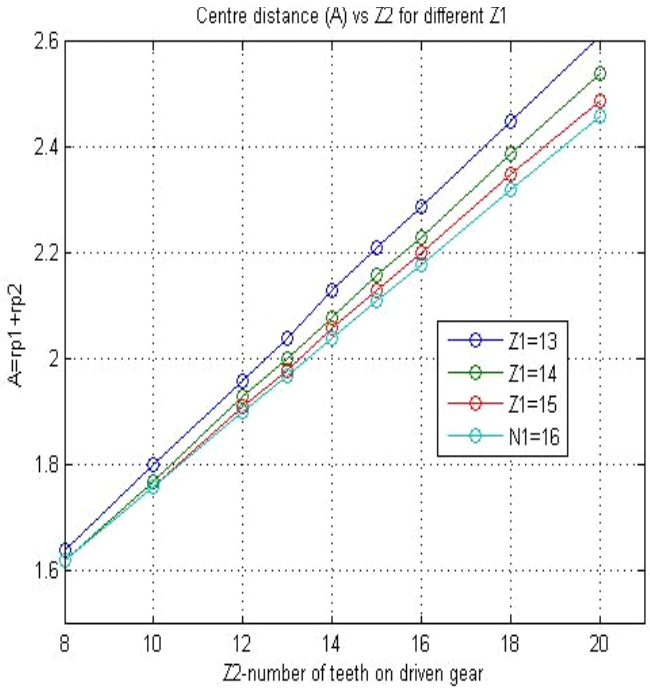


Fig 5 Plot between center distance and Z_2 for given Z_1

Instantaneous Flow Ripple The instantaneous flow ripple of the pump is given by the solution to Eq. (7). This solution is determined by solving for the length of action determined using the closed-form approximations using Matlab programming tool (Source codes in appendix A_M05_LN_22). Figure 6 shows a plot of the flow ripple calculation for the selected pumps, it can be seen that the amplitude of the flow ripple decreases significantly as the number of teeth on the driving gear increases.

Limiting values of θ

For Z1=13 θ=2π/13 = .4833
For Z1=14, θ=2π/14 = .4488
For Z1=15, θ=2π/15 = .4189
For Z1=16, θ=2π/16 = .3927
Once θ exceeds the limiting value then this value has to be subtracted from the desired angle because after this limiting value new teeth comes in contact

Flow Pulse Amplitude. The amplitude of the flow pulse is given by Eq. (23) Figure 7 shows a graph of the flow pulse amplitude as it varies with the numbers of teeth on both the driving and driven gears i.e. gear 1 and gear 2, respectively. This figure shows a strong dependence on the number of teeth on the driving gear. The flatness of the curves tends to show a weak dependence on the number of teeth on the driven gear.

Θ (rad)	Z_1=13, Z_2=16	Z_1=14, Z_2=15	Z_1=15, Z_2=16	Z_1=16, Z_2=13
0	.61	.69	.75	.80
.1	.84	.89	.93	.96
.2	1.01	1.03	1.04	1.05
.3	1.11	1.10	1.08	1.06
.4	1.16	1.11	1.06	1.01
.5	.65	.80	.91	1.05
.6	.87	.97	1.03	1.06
.7	1.03	1.08	1.08	1.03
.8	1.12	1.11	1.07	.83
.9	1.16	1.09	.876	.981
1	.664	.899	1.01	1.06

Table 2: Flow ripple at different angle of rotation of shaft.

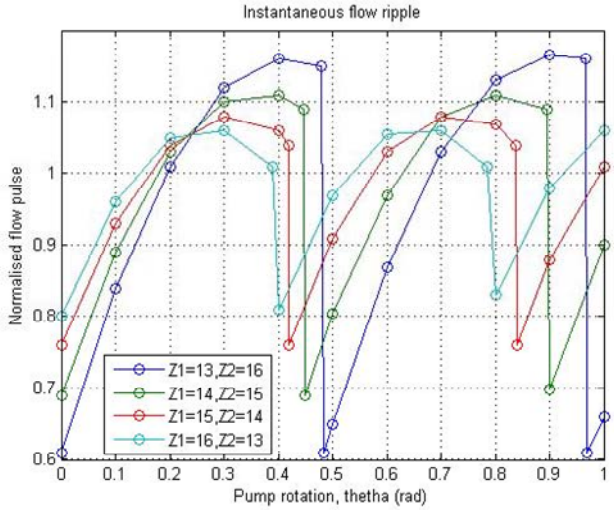


Fig. 6: Plot of Instantaneous Flow Ripple

3. Flow Pulse Amplitude

Flow Pulse Amplitude

$$\Delta \bar{Q}_d = \frac{1}{2}\left(1 + \frac{\bar{r}_{p1}}{\bar{r}_{p2}}\right)\bar{I}_s^{\,2}$$

Z_2	Z_1=13	Z_1=14	Z_1=15	Z_1=16
8	.635	.478	.377	.312
10	.603	.454	.356	.291
12	.584	.439	.341	.275
14	.570	.426	.329	.263
16	.560	.418	.320	.255
18	.550	.411	.312	.248
20	.542	405	307	.242

Table: 3. Flow pulse amplitude for Different numbers of teeth on driving and driven gears

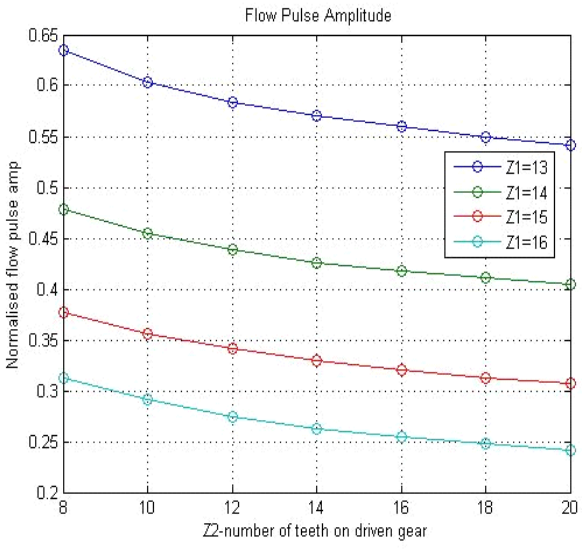


Fig.- 7: Plot of the flow pulse amplitude

Summary

The following conclusions are supported by the analysis and results.
1. To solve the instantaneous flow ripple equation of the gear pump, a numerical solution is generally required. However, a closed-form approximation for the flow ripple equation can be used without introducing significant error into the solution.
2. Reducing the numbers of teeth on the driven gear may be used to reduce the centre distance and physical pump size. This can be done without altering the average flow rate of the pump and without increasing the flow pulsation dramatically.
3. The centre distance can be reduced slightly by increasing the number of teeth on the driving gear as well. However, this impact is not as significant as the one noted in the item 2.
4. The pulse amplitude of the flow ripple is primarily determined by the number of teeth on the driving gear of the pump. By increasing the number of teeth on the driving gear, the flow pulse amplitude can be significantly reduced.
5. Increasing the number of teeth on the driven gear can also reduce the pulse amplitude of the flow ripple. However, this impact is not as significant as the one noted in the item 4.

In brief, results of this study show that it may be advantageous to design an external gear pump with a large number of teeth on the driving gear and a fewer number of teeth on the driven gear. This design configuration will tend to reduce both the physical pump size (without reducing the volumetric displacement of the pump) and the amplitude of the flow pulsation.

Bibliography:

1. Noah D Manring and Suresh B Kasaragadda "The Theoretical Flow Ripple of an External Gear Pump" Vol 25 Transaction of ASME pp 396-404.
2. J Ivantysyn, and M Ivantysynova "Hydrostatic Pumps and Motors", Akademia Books International, New Delhi ISBN-81-85522-16-2.
3. Yanzhi Li , Lihuan Gao and Xiaoyang Tang. "The flow pulsation analysis of an external gear pump", Advanced Materials Research Vols. 236-238 (2011) pp 2327-2331.
4. Frith R H, and Scott W 1996, ''Comparison of an external gear pump wear model with test data,'' Wear, **196**, pp. 64–71.
5. Chen Lipeng and Zhao Yan "Modelling and simulation of gear pump", Proceeding 8th Modilica conference, Dresden Germany ,March 2011 pp 421-428

Nomenclature

A = centre distance between shaft on gear pump
l = instantaneous length of action within the gear mesh
l_f = length of action within the gear mesh just prior to another set of teeth making contact
l_s = length of action within the gear mesh when the teeth make the first point of contact
$Z_{1,2}$ = number of teeth on the driving and driven gear

Q = volumetric flow rate
$r_{a1,2}$ = addendum radius of the driving and driven gear
$r_{b1,2}$ = base circle radius of the driving and driven gear
$r_{p1,2}$ = pitch radius of the driving gear and driven gear
V = volume
$V_{i1,2}$ = volume entering the control volume with the driving and driven gear
$V_{o1,2}$ = volume leaving the control volume with the driving and driven gear
w = width of the gear teeth
α = pressure angle
$\beta_{1,2}$ = angular dimension locating the instantaneous point of contact on the driving and driven gear
β_{1s} = angular dimension locating the point of contact on the driving gear when the teeth make the first point of contact
β_{1f} = angular dimension locating the point of contact on the driving gear just prior to another set of teeth making contact
$\theta_{1,2}$ = angular displacement of the driving and driven gear
θ_{1f} = angular displacement of the driving gear just prior to another set of teeth making contact
ξ = angular orientation of the fixed Cartesian coordinate system
$\rho_{1,2}$ = radial dimension locating the instantaneous point of contact on the driving and driven gear
ρ_{1f} = radial dimension locating the point of contact on the driving gear just prior to another set of teeth making contact
ρ_{1s} = radial dimension locating the point of contact on the driving gear when the teeth make the first point of contact
ψ_1 = half angle of the tooth width measured at the base circle of the driving gear

Involute Geometry of Gear. Referring to Fig. 8,

$$\rho = r_b\sqrt{1+\varphi^2} \text{ and } \beta = \psi - \varphi + \gamma . \tag{31}$$

The Cartesian transformation of these coordinates is as follows,

$$x = \rho\cos(\beta) \text{ and } y = \rho\sin(\beta) \tag{32}$$

Again, referring to fig.

$$r_b = \rho\cos(\gamma) \text{ and } r_b\varphi = \rho\sin(\gamma) \tag{33}$$

From above equations β can be derived as,

$$\beta = \psi - \sqrt{\left(\frac{\rho}{r_b}\right)^2 - 1} + \cos^{-1}\left(\frac{r_b}{\rho}\right). \tag{34}$$

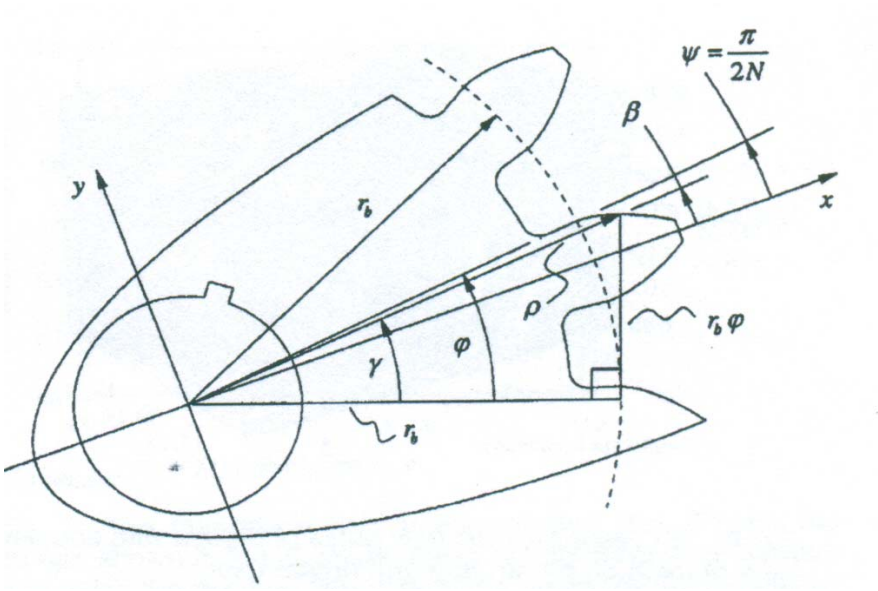


Fig.- 8: The involute geometry of a tooth profile.

Bibliography:

1. Noah D Manring and Suresh B Kasaragadda "The Theoretical Flow Ripple of an External Gear Pump" Vol 25 Transaction of ASME pp 396-404.
2. J Ivantysyn, and M Ivantysynova "Hydrostatic Pumps and Motors", Akademia Books International, New Delhi ISBN-81-85522-16-2.
3. Yanzhi Li , Lihuan Gao and Xiaoyang Tang. "The flow pulsation analysis of an external gear pump", Advanced Materials Research Vols. 236-238 (2011) pp 2327-2331.
4. Frith R H, and Scott W 1996, "Comparison of an external gear pump wear model with test data," Wear, 196, pp. 64–71.
5. Chen Lipeng and Zhao Yan "Modelling and simulation of gear pump", Proceeding 8th Modilica conference, Dresden Germany ,March 2011 pp 421-428.